ELSEVIER

Catalysis Today 41 (1998) 297–309

CATALYSIS TODAY

Photocatalyzed oxidation in zeolite cages

Fritz Blatter[1], Hai Sun[2], Sergey Vasenkov, Heinz Frei*

Physical Biosciences Division, MS Calvin Laboratory, Lawrence Berkeley National Laboratory, University of California, Berkeley, CA 94720, USA

Abstract

A new concept of room temperature selective oxidation of olefins, alkyl substituted benzenes and alkanes by electron transfer from the hydrocarbon to the oxygen molecule induced by irradiation with visible light is shown. The hydrocarbon radical cation–O_2 charge-transfer pair is generated inside the cavities of alkali or alkaline-earth ion-exchanged zeolites, in which the large electrostatic field stabilizes the highly polar charge-transfer states of hydrocarbon–O_2 collisional pair and allows to control the pathways of further transformation. High selectivities to useful products are obtained using this approach.

Keywords: Zeolites; Photooxidation; Alkanes; Alkylaromatics; Olefins

1. Introduction and background

Partial oxidation of small alkanes, alkenes, and aromatics is one of the most important processes in chemical industry. The products serve as building blocks for plastics and synthetic fibers, or as industrial intermediates in the manufacture of fine chemicals. Oxidation of low alkanes plays a central role in the use of natural gas and of volatile petroleum fractions as new feedstocks for industrial chemicals [1–6]. For these large scale processes, molecular oxygen is the only economically viable oxidant. Direct oxidations by O_2 are very unselective for most small hydrocarbons, however. As a result, existing methods generate large amounts of unwanted byproducts which require energy-intensive separation processes. The main reason for the lack of selectivity is the free radical nature of the gas or liquid phase processes, the high exothermicity of the reactions, and overoxidation. Unrestricted mobility of the free radical intermediates results in indiscriminate attack on starting hydrocarbon and primary oxidation products. Overoxidation is due to the fact that, under thermal conditions in liquid or gas phase, oxygen attacks partially oxidized products more easily than the starting hydrocarbon. The lack of control gets worse as products accumulate, limiting conversion to a few percent in most practical processes.

Recent efforts towards improvement of the selectivity of hydrocarbon oxidation by O_2 encompass a diverse spectrum of approaches. Low alkane oxidations are mainly based on catalysis over metal and mixed metal oxides [7–12], with some of these solids

*Corresponding author. Fax: +1-510-486-6059; e-mail: hmfrei@lbl.gov

[1]Present address: Novartis Services AG, CH-4002 Basel, Switzerland.

[2]Present address: International Rectifier, El Segundo, CA USA.

0920-5861/98/$32.00
PII S0920-5861(98)00021-2

acting mainly as oxidative dehydrogenation catalysts [13–16]. Mixed metal oxides play an important role in oxidation of unsaturated hydrocarbons as well [17]. Some solid oxides have shown to be effective oxidation catalysts under irradiation with UV light [18–24]. Electrochemical methods [25,26] and catalysis by transition metal complexes [6,27,28] are being explored. Although selectivities are dramatically improved over plain autoxidation, all these methods still generate substantial amounts of carbon oxides or other carbon fragmentation products, some even at low hydrocarbon conversion. Several groups have focused on porphyrin analogs of nature's monooxygenase enzymes that are capable of low alkane and olefin oxidation by O_2 to alcohols or epoxides [3,29]. Many porphyrin systems require sacrificial reducing agents [3], but some afford oxidation of even small hydrocarbons without the need of a stoichiometric reductant. These include perhalo iron porphyrins [30], UV light-assisted oxidation of alkanes in the presence of metalloporphyrins [31] and epoxidation of olefins by Ru porphyrin [32]. A most recent approach is oxidation in redox molecular sieves (metal aluminophosphates or metal silicates) [33–36]. Selectivities are high, but typically only at a few percent conversion of the hydrocarbon, a persistent problem in all existing methods using O_2 that is especially severe for low alkanes and alkenes.

2. Concept

A possible way of activating dioxygen and hydrocarbon is to induce electron transfer from the hydrocarbon to the oxygen molecule to form a radical cation and O_2^- (superoxide). Alkane or alkene radical cations so produced are extremely acidic and, therefore, have a strong tendency to transfer a proton to O_2^- to yield allyl (alkyl) and HOO radicals. While these are the same radicals produced in conventional liquid or gas phase autoxidation, generating them at ambient temperature in a restricted environment may offer ways to tightly control their fate and, hence, accomplish high selectivity in terms of final oxidation products.

Charge-transfer from alkane (or alkene, arene) to oxygen can be induced by absorption of a photon by a hydrocarbon–O_2 collisional complex or, in principle, spontaneously in a thermal process if molecules were occluded in a highly ionic environment. Light-induced formation of hydrocarbon–O_2 charge-transfer states has first been reported in the 1950s by the groups of Evans and Mulliken [37,38]. Optical absorptions in the UV region originating from transition to excited charge-transfer states of alkane, alkene, or arene–O_2 collisional pairs were observed in O_2-saturated hydrocarbon liquids and high-pressure O_2 gas phase. They appear typically as long, structureless absorption tails. Upon irradiation with UV light, photooxidation was observed and interpreted by a mechanism that features proton transfer from the hydrocarbon radical cation to O_2^- as the initial step [39–42]. However, these UV light-driven gas or liquid phase oxidations resulted in a multitude of products. The challenge of selective activation via charge-transfer between hydrocarbon and O_2 is to find a much milder way to generate the radical cation–O_2^- pair and some means to control the chemistry of the subsequently produced radicals and primary oxidation products.

A solvent-free cation-exchanged zeolite is an environment for hydrocarbon-oxygen gas phase photochemistry that offers a solution to both challenges. Zeolites are crystalline alumino-silicates with a network of molecular-size channels or cages [43]. These present diffusional constraints that may prevent undesired radical coupling reactions that dominate the chemistry in conventional fluid media. In addition, the poorly shielded extra-framework cations of alkali or alkaline-earth zeolites create large electrostatic fields in their vicinity that would strongly stabilize the highly polar charge-transfer states of hydrocarbon–O_2 collisional pairs with their dipole aligned parallel to the field. Such stabilization of the radical cation–O_2^- states may render them accessible to visible light at room temperature, or even to thermal excitation at modestly elevated temperatures. Use of long-wavelength visible instead of UV photons would guarantee generation of the primary photoproducts with the least amount of excess energy, thus minimizing homolytic bond rupture and random coupling reactions. Moreover, secondary photolysis leading to product decomposition and overoxidation would be prevented. We describe below several examples which demonstrate this new concept of selective oxidation of alkenes, alkanes, and alkyl substituted aromatic hydrocarbons.

3. Examples

3.1. Olefin oxidations

Visible light-induced oxidations of small olefins by O_2 studied thus far are displayed in Fig. 1. Among these, the reaction of 2,3-dimethyl-2-butene in alkali or alkaline-earth zeolites occurs at the fastest rate. Hence, this reaction served as a convenient system for addressing spectroscopic and mechanistic questions, which we will discuss in the form of an introductory example.

We chose zeolite Y (Si:Al=2.4) in its Na^+ or Ba^{2+}-exchanged form as a matrix host for most of our work. The structure of this material is in essence a 3-dimensional network of 13 Å spherical cages (called supercages) interconnected by windows of 8 Å diameter. Experiments were also conducted in some cases with K or Ba forms of zeolite L, a 1-dimensional structure of 7 Å diameter channels [43]. These are zeolites which can readily be prepared free of Brönsted or Lewis acid sites when dehydrated under mild conditions [44]. Loading of a self-supporting pressed pellet of 1 μm NaY crystallites (1 cm diameter, 50–100 μm thick) with 0.5 Torr olefin and 1 atm O_2 gas at ambient temperature resulted in 1–2 hydrocarbons per supercage and one O_2 every 3–4 supercages on average. Exposure of the zeolite to visible or near-infrared light at wavelengths as long as 750 nm induced oxidation of the olefin as detected by in situ FT-infrared spectroscopy [45–48]. An infrared spectrum of the product taken upon oxidation of >90% of the loaded 2,3-dimethyl-2-butene by visible light at −50°C is shown in Fig. 2 (for experiments below room temperature, the miniature infrared gas cell holding the pellet was mounted inside a variable-temperature vacuum system). The spectrum is that of the corresponding allyl hydroperoxide (2,3-dimethyl-3-hydroperoxy-1-butene) plus a small amount of acetone (about 2%), the established thermal decomposition product of this alkene hydroperoxide. Rates were 5×10^{-4} mol cm^{-3} h^{-1} for 1 W of green light which corresponds to a space-time yield of 0.05 mol cm^{-3} h^{-1} for irradiation of the 1 cm^2 pellet area with 100 W visible light. The same photooxidation was observed in zeolite BaY, KL, or BaL. Product

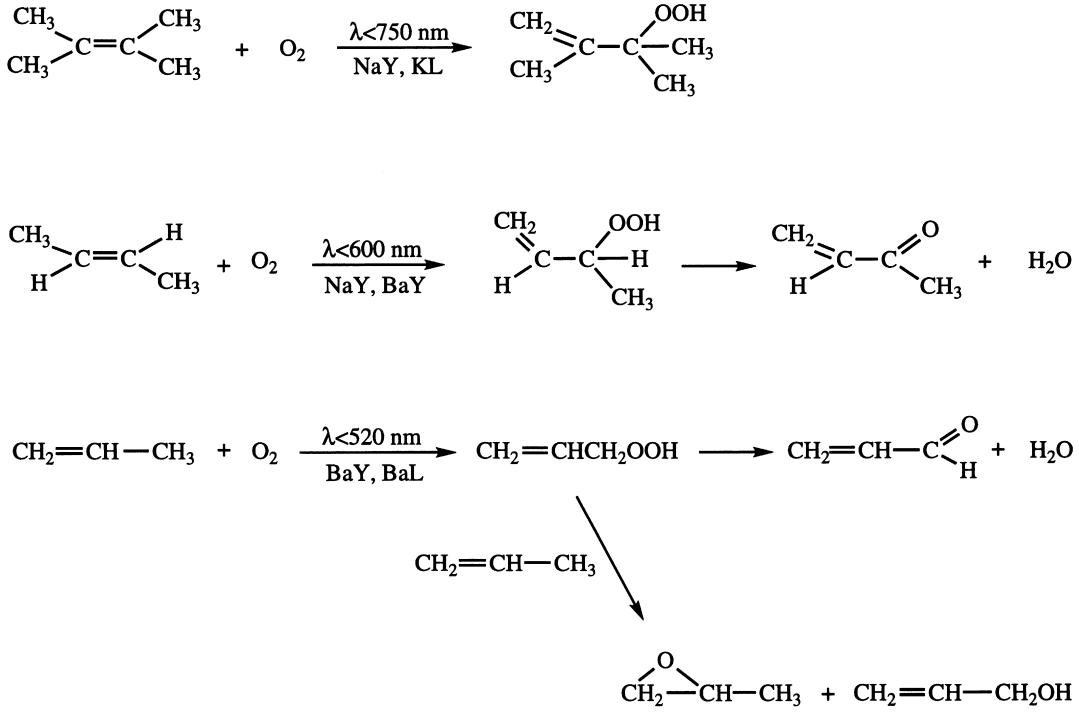

Fig. 1. Selective alkene photooxidations in cation-exchanged zeolite Y or L.

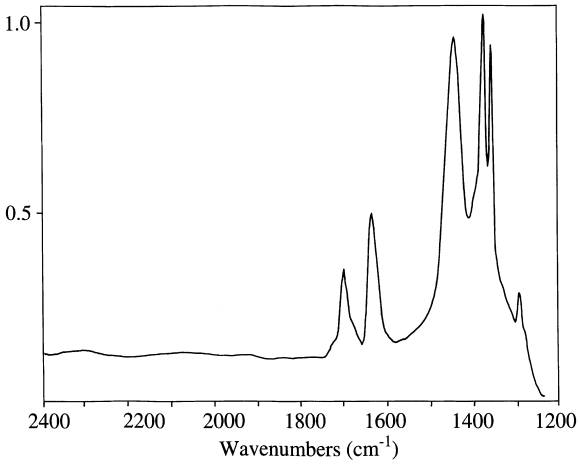

Fig. 2. Infrared product spectrum on >90% conversion of 2,3-dimethyl-2-butene and O_2 in zeolite NaY under visible light at −50°C. All absorptions originate from 2,3-dimethyl-3-hydroperoxy-1-butene except the band at 1708 cm^{-1}, which is due to acetone (2%).

and yield were independent of whether the visible output of a conventional tungsten lamp or the monochromatic emission of a continuous-wave visible laser was used for photolysis. Use of the laser was especially convenient for wavelength dependence studies.

Recording of an optical spectrum of the 2,3-dimethyl-2-butene and O_2-loaded NaY pellet reveals a weak continuous absorption tail in the visible extending into the red spectral region (Fig. 3) [49]. The spectrum appears only when both olefin and O_2 are present in the zeolite, hence originates from a

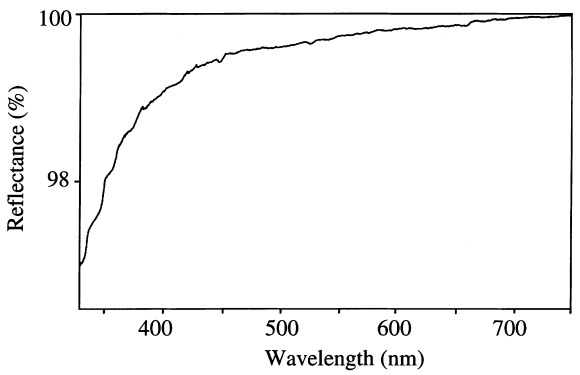

Fig. 3. UV–VIS reflectance spectrum of 2,3-dimethyl-2-butene and O_2 gas-loaded zeolite NaY at room temperature showing the alkene–O_2 charge-transfer absorption tail.

hydrocarbon–O_2 collisional complex. This absorption is responsible for the light-induced oxidation of the olefin. The highly scattering nature of the pressed zeolite pellet in the UV–VIS region required measurement of the optical spectrum in the reflectance mode with an integrating sphere. The steep increase of the absorption towards shorter wavelengths, especially at λ<400 nm is attributed to a longer path of the light due to increased scattering. While this effect is beneficial in terms of photochemical product yields, it obscures the true shape of the visible olefin–O_2 absorption. We have very recently succeeded in preparing optically transparent monolayers of large (40 μm) NaY crystals on a CaF_2 support. The sharply reduced scattering of these layers allowed us to record the true absorption profile, which features a shallow maximum between 400 and 500 nm [50].

The zeolite (cation) dependence of the absorption and the relationship between its onset and the ionization potential of the hydrocarbon indicate that the visible absorption is due to a hydrocarbon–O_2 contact charge-transfer transition [49]. On absorption of a photon by an olefin–O_2 collisional complex, an electron is transferred from the hydrocarbon to oxygen, resulting in the formation of alkene radical cation and O_2^-. For 2,3-dimethyl-2-butene–O_2 in the liquid hydrocarbon or gas phase, the charge-transfer absorption tail starts around 400 nm [51,52]. According to Fig. 3, this implies a very large red shift of 350 nm for the olefin–O_2 absorption in NaY, indicating a strong stabilization of the excited charge-transfer state by the zeolite cage.

Such a strong stabilization of an alkene$^+$–O_2^- charge-transfer pair inside a zeolite cage is expected to arise from the interaction of its large dipole (about 15 Debye) with the high electrostatic field in the vicinity of alkali or alkaline-earth cations. In the case of NaY and BaY, the zeolites most frequently used in our experiments, there are 3–4 cations located in each supercage [43]. The wall of the cage carries a formal negative charge of 7 which resides on the framework oxygens. The electric shielding of the cations in the supercage by the framework oxygen is poor, resulting in high electrostatic fields around the cations. There is extensive experimental evidence for the existence of such electrostatic fields in cation-exchanged zeolites from infrared [53–56] and ESR spectroscopy [57,58] of small guest molecules, from electron densities

determined by X-ray measurements [59], and from heat of adsorption measurements of rare gases [60]. Model and ab initio calculations confirm these results [61–63]. We have employed the infrared method for estimating field strengths in the zeolites used for hydrocarbon oxidations. Fig. 4 shows the infrared absorption of the fundamental vibration of N_2 gas occluded in zeolite NaY, BaY, KL and BaL. This transition is infrared inactive for the free gas, but gains intensity in the vicinity of a poorly shielded cation because of the dipole induced by the electrostatic field. Intensities are proportional to the square of the field strength experienced by the molecule, and values of 0.3 and 0.9 $V\,Å^{-1}$ were derived from such measurements for NaY and BaY, for example [64]. The interaction of the high electrostatic field with the large dipole generated upon excitation of the olefin–O_2 pair to the charge-transfer state results in a stabilization of the excited state by 1.5 eV for orientation parallel to the field (generally between 1 and 3 eV depending on hydrocarbon and exchanged cation). The result is a very large red shift of the absorption from the UV into the visible region. Hence, it is this electrostatic field effect of the zeolite cage on the charge-transfer absorption that allows us to access hydrocarbon oxidation by visible light. This is an effect of the zeolite medium with every cage capable of contributing to the photoreaction.

The initial step of the proposed mechanism is proton transfer from the alkene radical cation, formed by photoexcitation, to O_2^- (Fig. 5).

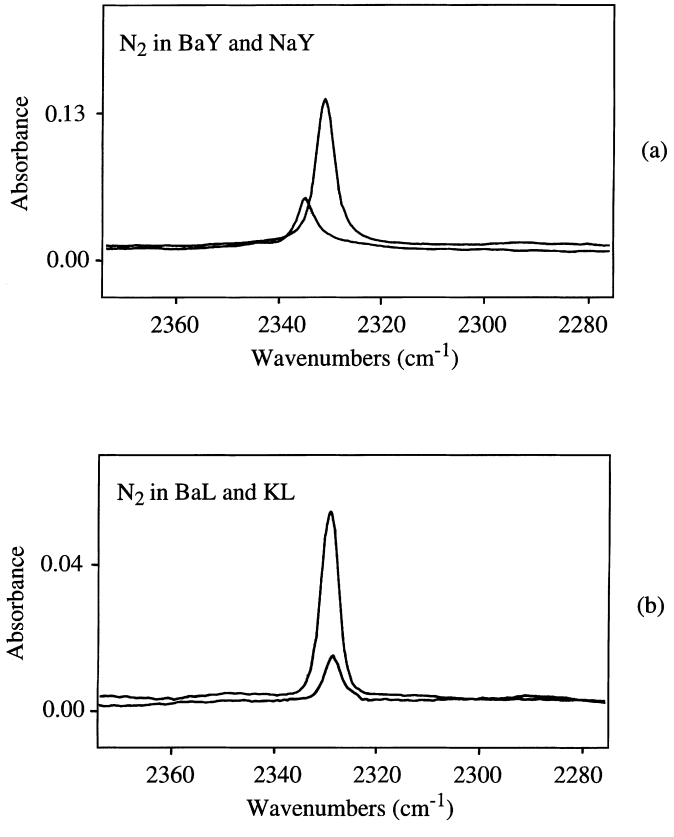

Fig. 4. Infrared absorption of N_2 induced by the electrostatic field in the vicinity of cations in zeolites Y and L. (a) Zeolite Y. Large band, BaY; small band, NaY. The spectra were recorded at 195 K, and the loading level corresponds to 1.3 N_2 molecules per supercage. (b) Zeolite L. Large signal, BaL (80% of K^+ exchanged by Ba^{2+}); small signal, KL. The spectra were recorded at 123 K, and the N_2 concentration was the same in the two zeolites.

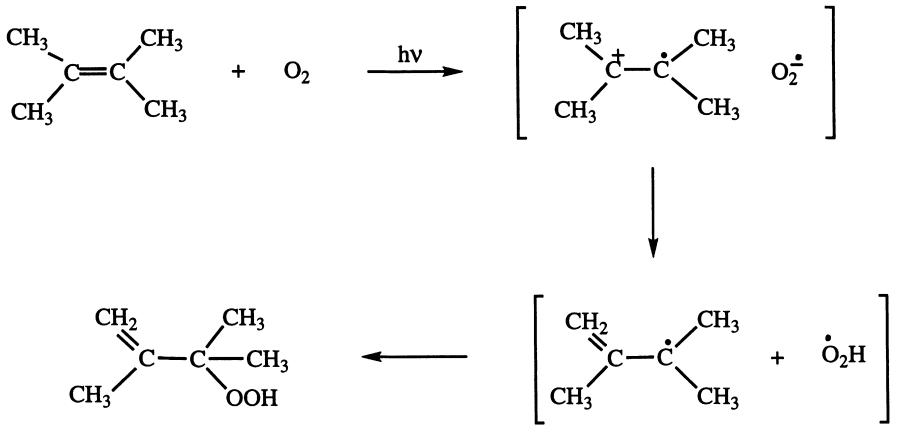

Fig. 5. Proposed mechanism for alkene photooxidation.

Radical cations of small olefins are spectroscopically established transients, and some have been previously observed in zeolites [65]. Proton transfer from the radical cation to O_2^- is expected to be very fast because of the high acidity of the cations. Efficient proton transfer quenching of the charge-transfer pair is probably the main reason for the rather high quantum yields to reaction of the hydrocarbon photooxidations (typically between 0.1 and 0.3, defined as product growth per absorbed photon) [49] because it furnishes a path that is competitive with back electron transfer. The allyl and hydroperoxy radical so produced lie approximately 40 kcal mol^{-1} above olefin+O_2 [66] and are expected to undergo fast cage recombination to yield the observed allyl hydroperoxide.

A partial olefin oxidation of commercial importance is that of propylene. Selectivity is a particularly tough challenge for this small alkene. Irradiation of propylene and O_2-loaded zeolite BaY at room temperature with green or blue light induced partial oxidation of the olefin [67]. The need for shorter wavelength photolysis light compared to 2,3-dimethyl-2-butene oxidation reflects the higher ionization potential of propylene (9.7 versus 8.3 eV). Readily identified products were acrolein, allyl hydroperoxide, and propylene oxide (Fig. 1). The hydroperoxide was found to be stable when the zeolite was kept at low temperature (−100°C). Hence, photolysis experiments at this temperature allowed us to elucidate the origin of aldehyde and epoxide product. Allyl hydroperoxide was the main product at −100°C, the remaining 13% were propylene oxide. Warm-up of the zeolite after photo-accumulation of the hydroperoxide produced propylene oxide if excess propylene was kept in the matrix, but only acrolein if the olefin was removed prior to warm-up. Therefore, allyl hydroperoxide is the primary photoproduct and acrolein originates from dehydration of the hydroperoxide. Propylene oxide, on the other hand, is produced by dark O transfer from allyl hydroperoxide to excess olefin (Fig. 1). We found that thermal rearrangement of the hydroperoxide to acrolein exhibits a steep temperature dependence while the epoxidation reaction does not. Hence, the aldehyde is the preferred final oxidation product of the visible light-driven propylene oxidation at elevated zeolite temperature. For example, when conducting the propylene+O_2 photoreaction at 55°C, the acrolein to propylene oxide ratio is 2 to 1. Variation of the propylene loading level gives an additional handle on the acrolein/propylene oxide branching.

The most important result of propylene photooxidation by visible light in zeolite is the unprecedented selectivity in terms of the allyl hydroperoxide intermediate (>98% at ambient temperature). The selectivity is undiminished even upon consumption of 20% of the propylene loaded into the zeolite. On the basis of spectroscopy of the visible propylene–O_2 charge-transfer absorption and the measured infrared product growth, a rather high reaction quantum efficiency of 20% was estimated. Essentially identical results were obtained with this reaction in zeolite BaL.

3.2. Alkyl substituted benzenes

Partial oxidation of toluene to benzaldehyde by O_2 is a long-standing challenge of commercial importance [1]. The aldehyde is an industrial intermediate for the manufacture of agrochemicals, flavors, and fragrances. Yet, there is currently no process that would oxidize toluene by O_2 to benzaldehyde selectively.

Using the photochemical and infrared probing techniques described above for the study of the visible light-induced alkene oxidations, we found that toluene reacts with O_2 in zeolite BaY or CaY at λ<600 nm to form benzaldehyde (and H_2O) without byproduct [68]. When we ran the photoreaction while the zeolite pellet was held at −60°C, benzyl hydroperoxide was trapped [69]. Warm-up of the matrix to room temperature resulted in spontaneous dehydration to benzaldehyde, indicating that the hydroperoxide is a reaction intermediate (Fig. 6). Complete selectivity was sustained even upon conversion of as much as half of the toluene loaded into the zeolite. An infrared difference spectrum recorded after 30% conversion of the loaded toluene is shown in Fig. 7. In particular, no overoxidation to benzoic acid occurred, which is the main problem in Co(III) catalyzed autoxidation of toluene currently practiced [1]. Overoxidation of benzaldehyde in the case of the visible light-driven reaction in the zeolite is prevented because the ionization potential of the aldehyde (9.5 eV) is higher than that of toluene (8.8 eV). Therefore, the benzaldehyde–O_2 charge-transfer absorption does not extend into the visible region, making it inaccessible to photolysis light. As a result, no further oxidation to benzoic acid can occur. In a similar study, partial oxidation of ethyl benzene to acetophenone was achieved in BaY with complete selectivity [69].

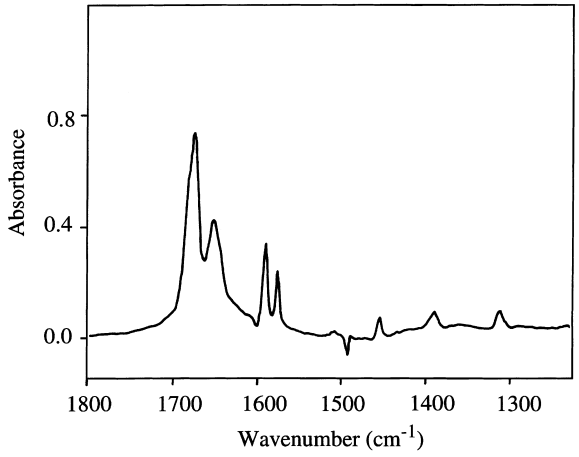

Fig. 7. Infrared difference spectrum upon 30% conversion of toluene and O_2 in zeolite BaY with visible light at ambient temperature. Benzaldehyde and H_2O are the only final oxidation products.

While the selectivity of these partial oxidations by O_2 is unprecedented, the strong physisorption of the polar carbonyl products inside the zeolite pores poses a challenge. Conditions have to be found that would allow product desorption from the zeolite at acceptable rates. This may involve a gas flow approach at moderately elevated zeolite temperature. Zeolites with

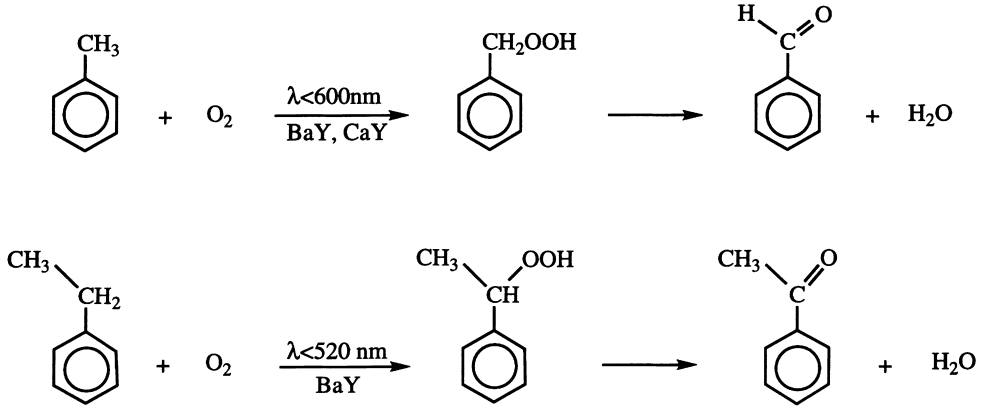

Fig. 6. Selective oxidation of alkyl benzenes under visible light in alkaline-earth zeolite Y.

lower Al content (hence lower concentration of exchangeable alkali or alkaline-earth cations) are expected to desorb polar products more easily. On the other hand, these cations are needed for generating the electrostatic fields that shift the hydrocarbon–O_2 absorption band into the visible. Hence, the task is to seek an optimum Si/Al ratio that satisfies both the need for charge-transfer stabilization and fast product desorption.

3.3. Selective oxidation of alkanes

Visible light-induced oxidation: Comparison of ionization potentials of alkanes with those of low alkenes suggests that visible light-induced oxidation through charge-transfer chemistry ought to be feasible for alkanes as well. For example, the ionization potential of cyclohexane (9.8 eV) is practically the same as that of propylene (9.7 eV). Indeed, reflectance spectroscopy of cyclohexane and O_2-loaded zeolite NaY revealed a continuous absorption tail with an onset around 500 nm [70]. Green or blue light-induced partial oxidation of this and other alkanes as small as ethane were observed in zeolite BaY and CaY. Reactions which were studied in detail are summarized in Fig. 8 [70–72]. Alkyl hydroperoxides appeared as primary photoproducts. Quantum efficiencies, where they could be estimated, were found to be rather high, of the order of 0.1. The dependence of photochemical yields on alkane ionization potential and zeolite cation field indicates that excitation of the alkane–O_2 charge-transfer state is responsible for these oxidations. Red shifts of the absorption relative to the gas or liquid phase are again on the order of 2–3 eV. Particularly exciting is the finding that all these visible light-driven partial oxidations proceed with complete selectivity even at high (>50%) conversion of the alkane. Specifically, no carbon oxide byproducts were observed, not even in the case of propane or ethane. All carbonyl products are important organic building blocks or industrial intermediates. The approach opens up the possibility of using ethane and propane, both constituents of natural gas, as new feedstocks for acetaldehyde and acetone in place of petroleum-derived ethylene and propylene currently used. In the case of *t*-butyl hydroperoxide, an oxidizing reagent, we

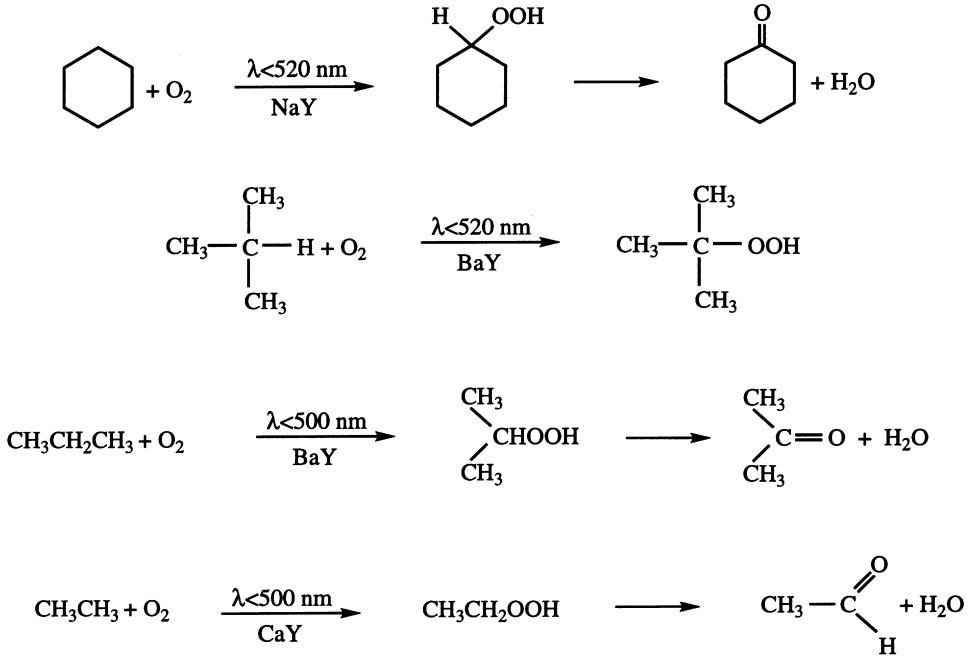

Fig. 8. Selective photooxidation of small alkanes by O_2 in alkali and alkaline-earth zeolite Y.

have demonstrated its in situ use in the zeolite for stereospecific dark epoxidation of *cis* or *trans*-2-butene [71].

A representative example of low alkane oxidations is that of propane [72]. When loading a room temperature pellet of zeolite BaY with 150–300 Torr propane and 1 atm of O_2 gas and exposing it to blue or green light from either a tungsten lamp or a continuous-wave laser, infrared product growth signaled the formation of acetone and H_2O as final products. A set of additional bands was identified as isopropyl hydroperoxide. The hydroperoxide spectrum decreased in the dark under concurrent formation of acetone and H_2O, indicating that it is formed as the primary photoproduct. Experiments with perdeuterated propane confirmed these conclusions.

The proposed mechanism for propane photooxidation, shown in Fig. 9, is entirely analogous to that for olefin oxidation (Fig. 5). Alkane radical cations generated upon photo-excitation are spectroscopically observed species that have a very high propensity for deprotonation to form alkyl radicals [73]. The alkyl hydroperoxide emerging from alkyl and HOO radical recombination dehydrates spontaneously in the ionic zeolite environment via a heterolytic mechanism [74]. This heterolytic H_2O elimination leads to carbonyl product without side reaction, in sharp contrast to homolytic peroxide bond rupture which is operative in conventional gas or solution phase autoxidation [1]. The use of low-energy photons and a low temperature environment precludes homolysis of the peroxide bond in the zeolite. This is an important point because the very reactive alkoxy and OH radicals formed upon alkyl hydroperoxide homolysis degrade product selectivity through indiscriminate attack on starting hydrocarbon and primary oxidation products even at low hydrocarbon conversion [1].

Thermal Oxidation: The charge-transfer mechanism of the visible light-induced oxidations in zeolites suggests that reactions could, in principle, be induced in the dark if electrostatic fields and thermal energies were sufficiently high to render the hydrocarbon radical cation– O_2^- state accessible in the absence of light. We have observed such dark thermal oxidation of 3 low alkanes, namely cyclohexane in NaY [70], isobutane in BaY at T>30°C, propane in BaY at T>50°C, and in CaY even at room temperature [72]. Oxidation products were cyclohexanone, *t*-butyl

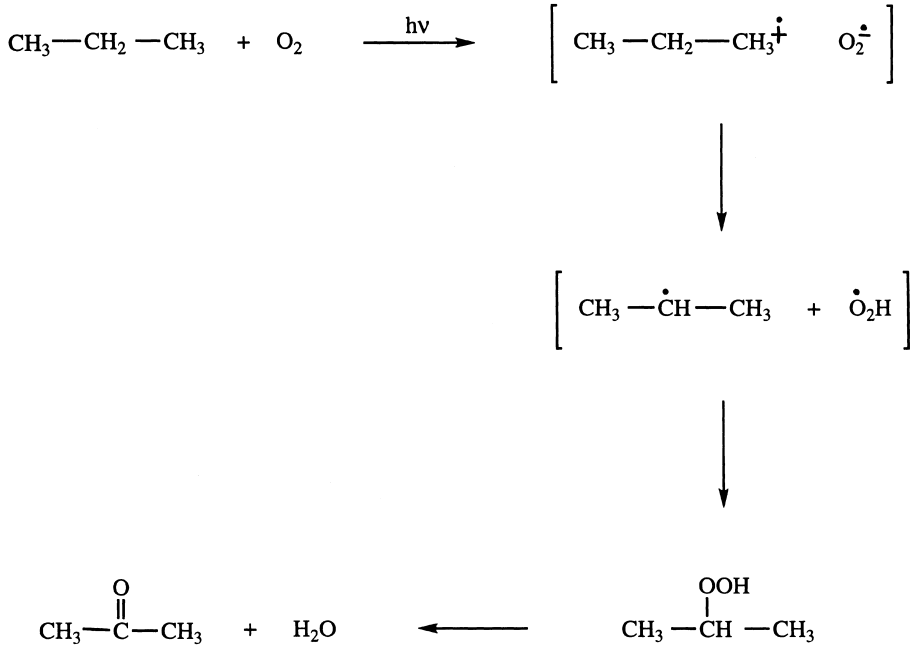

Fig. 9. Proposed mechanism for alkane photooxidation.

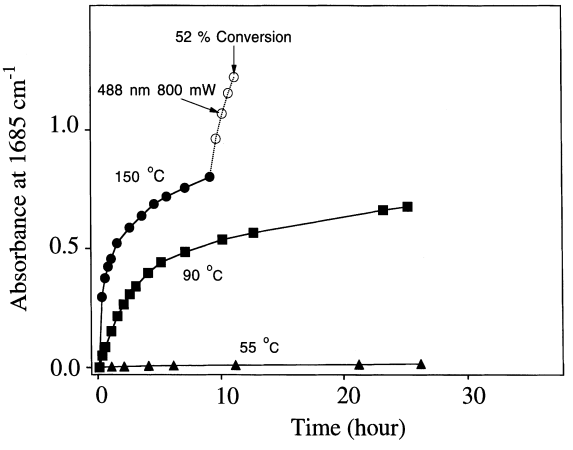

Fig. 10. Thermal propane oxidation by O_2. Curve 1 shows the acetone growth at 55°C, curve 2 at 90°C. Curve 3 represents thermal growth at 150°C (filled circles), followed by blue light-induced oxidation (open circles).

hydroperoxide, and acetone, respectively. As in the case of the photo-induced oxidation, selectivity was complete even at high conversion (>30%). Temperatures in our experiments did not exceed 80°C for cyclohexane in NaY, or 150°C in the case of propane in BaY. For illustration, the acetone growth kinetics upon thermal oxidation of propane in BaY is shown in Fig. 10 at three different temperatures. While the reaction is very slow at 55°C, rates increase sharply at 90 and 150°C. At 150°C, one third of the loaded propane is converted in 9 h, with acetone as the exclusive product. Subsequent irradiation with blue light for another 2 h continued to produce acetone, reaching 52% conversion of the alkane without side reaction. The steep slope of the growth curve clearly shows that there is no sign of leveling off even at this high conversion.

Several observations support explanation of the dark oxidation by the charge-transfer path proposed for the photo-induced reaction (Fig. 9) [72]. One such observation is that only cyclohexane, but not propane, is thermally oxidized in zeolite NaY. This is consistent with the considerably lower ionization potential of cyclohexane (9.8 eV) compared to propane (11.1 eV). Another finding is that propane reacts faster in CaY than in BaY, and not at all in NaY, consistent with the increasing fields NaY<BaY<CaY. We also found that increased concentration of residual H_2O gradually quenches the thermal reaction, which probably reflects shielding of the Coulombic interactions by water molecules adsorbed on the cations. All these observations support charge transfer from alkane to O_2 as the initial reaction step. It is possible that, at elevated temperatures, the familiar chain propagation (alkyl radical adding to O_2 to form peroxy radical, followed by H abstraction from alkane to yield alkyl hydroperoxide plus another alkyl radical) plays a role because sufficient energy is available to overcome the activation energy for H abstraction from the alkane [75].

It is interesting that unsaturated hydrocarbons such as low olefins or toluene do not exhibit thermal oxidation despite the fact that ionization potentials and C–H bond energies are appreciably smaller than for low alkanes. We attribute this to the strong interaction of olefins and benzenes with exchanged cations in the supercage. As a result, the hydrocarbons reside at these cations, especially those which are most poorly shielded by the framework oxygens [76,77]. Hydrocarbons adsorbed on cations are unable to undergo charge transfer with O_2 since the dipole of the contact complex is antiparallel to the electrostatic field. The diminished electrostatic fields of the olefin or benzene-shielded cations experienced by other collisional pairs may be too weak to promote thermal charge transfer between these hydrocarbon and O_2 molecules. By contrast, trajectories of diffusing alkane molecules are not following the cation sites [78,79]; hence, the alkane–O_2 collisional pairs experience the full electrostatic field of the unshielded cations.

There are two reports by other research groups on thermal alkane oxidation by O_2 gas in cation exchanged zeolite Y. Ukharskii et al. noted infrared product absorptions in the 1700–1800 cm^{-1} region upon oxidation of cyclohexane in NaY at temperatures as low as 60–80°C, indicating ketone and other products (possibly anhydride) [80]. Jacobs' group conducted very recently a systematic study of cyclohexane autoxidation in alkali and alkaline-earth zeolite Y (NaY, BaY, SrY, CaY) at 80°C [81]. Increased reactivity was observed in that order, and in situ monitoring by diffuse reflectance FT-IR revealed cyclohexanone and H_2O as initial products. Continued reaction resulted in growth at 1580 cm^{-1} assigned to a carboxylate product. While we have not observed any loss of product selectivity at the moderate temperatures used in our work, increase of the

zeolite temperature or use of cations with larger fields (e.g., Mg^{2+}) to achieve higher reaction rates may lead to steady-state concentrations of alkyl peroxy radicals that are sufficiently high to cause self-coupling of these intermediates. This might result in loss of product selectivity by concurrent formation of alcohols along with carbonyl products.

4. Possible extensions of the concept

In a broader context, the charge-transfer photochemistry of hydrocarbon–O_2 collisional pairs in alkali or alkaline-earth zeolite cages constitutes an example of supramolecular photochemistry [82,83]. The crucial functions of the supramolecular host (zeolite) in this case are (i) strong adsorption of the reactant gases leading to a high steady-state concentration of hydrocarbon–O_2 collisional pairs; (ii) high electrostatic fields exerted on these pairs in the vicinity of exchangeable cations, which strongly affects the energy of excited charge-transfer states and thereby opens up a low-energy oxidation path accessible by visible photons; (iii) motional constraints imposed on the proposed primary radical products (alkyl (allyl, benzyl) radical, HOO radical). This suppresses random radical coupling reactions which otherwise would destroy product selectivity.

With these key factors for selective hydrocarbon+O_2 charge-transfer photochemistry identified, it is clear that not just cation-exchanged zeolites, but any solid matrix host with microporous structure and sites of high electrostatic fields may be suitable for partial hydrocarbon oxidation. This may include organic polymeric materials with ions or ionic functional groups inside nanometer-size cavities, or non-zeolite inorganic microporous frameworks featuring exchangeable cations. The motivation for expanding the scope of microporous solid hosts is the improvement of desorption rates of the polar oxidation products (carbonyls, H_2O), as already alluded to in Section 3.2. Desorption properties can be influenced by the chemical make-up of the cage walls. Pore sizes should, however, remain on the nanometer scale because diffusional restriction on reaction intermediates is essential for high product selectivity.

Selection of new microporous materials for visible light-driven partial oxidations would be greatly aided by detailed knowledge about elementary reaction steps and their kinetics. Specifically, what is the lifetime of the proposed allyl (alkyl, benzyl) and HOO radicals? What structural features of the zeolite influence the lifetime and mobility of these intermediates? While there is a fast growing body of data on the diffusional properties of closed shell molecules based on pulsed field gradient NMR measurements [78], there is a paucity of information on diffusional behavior and lifetimes of radical intermediates in microporous solids. We are currently trying to monitor such transients on the nanosecond to millisecond time scale using step-scan and rapid scan FT-infrared spectroscopy [84]. There is a need for studies with complementary techniques, such as time-resolved EPR spectroscopy to broaden the scope of our understanding of key elementary processes in microporous solids.

Charge-transfer photochemistry of collisional complexes in zeolites need not be limited to hydrocarbon–O_2 systems. One can envision, for example, similar light-induced reactions in high electrostatic field environments involving hydrocarbon–CO_2 or hydrocarbon–N_2 contact complexes, reactions of obvious relevance to the activation of these inert molecules.

5. Conclusions

Chemo and regioselectivity in partial oxidation of small hydrocarbons by O_2 is a formidable challenge. Charge-transfer photochemistry with visible light in zeolites described in this paper has several ingredients that render the process selective. The most important aspect is the stabilization of the hydrocarbon radical cation–O_2^- charge-transfer pair by electrostatic interaction with the zeolite, which lowers substantially the energy needed to activate dioxygen and hydrocarbon. A second feature is the low (ambient) temperature at which the oxidation is conducted, thus avoiding homolytic OO bond rupture of the primary hydroperoxide product. As a result, no highly reactive radicals are generated that would destroy the selectivity. In the case of unsaturated hydrocarbons, overoxidation of primary products is blocked because the ionization potential of partially oxidized alkenes or alkyl benzenes (and therefore their charge-transfer state with O_2) is higher than that of the starting hydrocarbon.

Constraints of the zeolite environment on the mobility of the reaction intermediates contribute, no doubt, in a significant way to the high selectivity of these oxidations. Time-resolved spectroscopic studies are needed to elucidate the precise role of these constraints.

Acknowledgements

This work was supported by the Director, Office of Energy Research, Office of Basic Energy Sciences, Chemical Sciences Division of the U.S. Department of Energy under Contract No. DE-AC03-76SF00098. The authors thank Dr. Suk Bong Hong, Korean Institute of Science and Technology, for a generous supply of zeolite KL and BaL.

References

[1] R.A. Sheldon, J.K. Kochi, Metal-Catalyzed Oxidation of Organic Compounds, chap. 11, Academic Press, New York, 1981.
[2] C.B. Dartt, M.E. Davis, Ind. Eng. Chem. Res. 33 (1994) 2887.
[3] C.L. Hill (Ed.), Activation and Functionalization of Alkanes, Wiley, New York, 1989.
[4] J.E. Lyons, G.W. Parshall, Catal. Today 22 (1994) 313.
[5] G. Centi, Catal. Lett. 22 (1993) 53.
[6] R.A. Sheldon, R.A. van Santen (Eds.), Catalytic Oxidation, Principles and Applications, World Scientific Publishing, Singapore, 1995.
[7] Y.C. Kim, W. Ueda, Y. Moro-oka, Appl. Catal. 70 (1991) 175.
[8] N. Mizuno, M. Tateishi, M. Iwamoto, Appl. Catal. 128 (1995) L165.
[9] Y. Takita, H. Yamashita, K. Moritaka, Chem. Lett., (1989) 1733.
[10] W. Ueda, Y. Suzuki, Chem. Lett., (1995) 541.
[11] K. Otsuka, Y. Uragami, M. Hataro, Catal. Today 13 (1992) 667.
[12] M. Ai, J. Catal. 101 (1986) 389.
[13] S.T. Oyama, A.M. Middlebrook, G.A. Somorjai, J. Phys. Chem. 94 (1990) 5029.
[14] A. Erdöhelyi, F. Solymosi, J. Catal. 123 (1990) 31.
[15] Y.S. Yoon, N. Fujikawa, W. Ueda, Y. Moro-oka, K.W. Lee, Catal. Today 24 (1995) 327.
[16] R. Grabowski, B. Grzybowska, A. Kozlowska, J. Stoczynski, K. Wcislo, Y. Barbaux, Topics Catal. 3 (1996) 277.
[17] J.S. Yoo, Appl. Catal. A 143 (1996) 29.
[18] K. Marcinkowska, S. Kaliaguine, P.C. Roberge, J. Catal. 90 (1984) 49.
[19] K. Wada, K. Yoshida, Y. Watanabe, T. Suzuki, J. Chem. Soc. Chem. Commun., (1991) 726.
[20] N. Djeghri, M. Formenti, F. Juillet, S.J. Teichner, Faraday Disc. Chem. Soc. 58 (1974) 185.
[21] H. Yoshida, T. Tanaka, M. Yamamoto, T. Funabiki, S. Yoshida, J. Chem. Soc. Chem. Commun., (1996) 2125.
[22] M. Anpo, T. Suzuki, Y. Yamada, Y. Otsuji, E. Gianello, M. Che, in: G. Centi, F. Trifiro (Eds.), New Developments in Selective Oxidation, Elsevier, Amsterdam, 1990, p. 683.
[23] P. Pichat, J.M. Herrmann, J. Disdier, M.N. Mozzanega, J. Phys. Chem. 83 (1979) 3122.
[24] W. Mu, J.M. Herrmann, P. Pichat, Catal. Lett. 3 (1989) 73.
[25] T. Hayakawa, K. Sato, T. Tsunoda, K. Suzuki, M. Shimizu, K. Takehira, J. Chem. Soc. Chem. Commun., (1994) 1743.
[26] K. Otsuka, T. Ushiyama, I. Yamanaka, K. Ebitani, J. Catal. 157 (1995) 450.
[27] A. Sen, M.A. Benvenuto, M. Lin, A.C. Hutson, N. Basickes, J. Am. Chem. Soc. 116 (1994) 998.
[28] I.P. Stolarov, M.N. Vargaftik, D.I. Shishkin, I.I. Moiseev, J. Chem. Soc. Chem. Commun., (1991) 938.
[29] R.A. Sheldon (Ed.), Metalloporphyrins in Catalytic Oxidations, Marcel Dekker, New York, 1994.
[30] J.E. Lyons, P.E. Ellis, Jr., in ref. 29, Chap. 10.
[31] A. Maldotti, C. Bartocci, R. Amadelli, E. Polo, P. Battioni, D. Mansuy, J. Chem. Soc. Chem. Commun., (1991) 1487.
[32] J.T. Groves, R. Quinn, J. Am. Chem. Soc. 107 (1985) 5790.
[33] S.S. Lin, H.S. Weng, Appl. Catal. A 105 (1993) 289.
[34] D.L. Vanoppen, D.E. DeVos, M.J. Genet, P.G. Rouxlet, P.A. Jacobs, Angew. Chem. Int. Ed. Engl. 34 (1995) 560.
[35] J.D. Chen, R.A. Sheldon, J. Catal. 153 (1995) 1.
[36] G. Centi, F. Trifiro, Appl. Catal. A 43 (1996) 3.
[37] D.F. Evans, J. Chem. Soc., (1953) 345.
[38] H. Tsubomura, R.S. Mulliken, J. Am. Chem. Soc. 82 (1960) 5966.
[39] K.S. Wei, A.H. Adelman, Tetrahedron Lett., (1969) 3297.
[40] J.C.W. Chien, J. Phys. Chem. 69 (1965) 4317.
[41] K. Onodera, G. Furusawa, M. Kojima, M. Tsuchiya, S. Aihara, R. Akaba, H. Sakuragi, K. Tokumaru, Tetrahedron 41 (1985) 2215.
[42] N. Kulevsky, P.V. Sneeringer, L.D. Grina, V.I. Stenberg, Photochem. Photobiol. 12 (1970) 395.
[43] D.W. Breck, Zeolite Molecular Sieves: Structure, Chemistry and Use, Wiley, New York, 1974.
[44] J.A. Rabo, Catal. Rev. 23 (1981) 293.
[45] F. Blatter, H. Frei, J. Am. Chem. Soc. 115 (1993) 7501.
[46] F. Blatter, H. Frei, J. Am. Chem. Soc. 116 (1994) 1812.
[47] H. Frei, F. Blatter, H. Sun, CHEMTECH 26 (1996) 24.
[48] H. Sun, F. Blatter, H. Frei, in: S.T. Oyama, B.K. Warren (Eds.), Heterogeneous Hydrocarbon Oxidation, ACS Symposium Series No. 638, American Chemical Society, Washington, D.C., 1996, p. 409.
[49] F. Blatter, F. Moreau, H. Frei, J. Phys. Chem. 98 (1994) 13403.
[50] S. Vasenkov, H. Frei, J. Phys. Chem. B 101 (1997) 4539.
[51] J.W. Coomber, D.M. Hebert, W.A. Kummer, D.E. Marsh, J.N. Pitts Jr., Environ. Sci. Technol. 4 (1970) 1141.
[52] M. Itoh, R.S. Mulliken, J. Phys. Chem. 73 (1969) 4332.
[53] B. Barrachin, E. Cohen de Lara, J. Chem. Soc., Faraday Trans. 2(82) (1986) 1953.

[54] G.H. Smudde, T.L. Slager, C.G. Coe, J.E. MacDougall, S.J. Weigel, Appl. Spectrosc. 49 (1995) 1747.
[55] C.L. Angell, P.C. Schaffer, J. Phys. Chem. 70 (1966) 1413.
[56] A. Zecchina, S. Bordiga, C. Lamberti, G. Spoto, L. Carnelli, J. Phys. Chem. 98 (1994) 9577.
[57] J.A.R. Coope, C.L. Gardner, C.A. McDowell, A.I. Pelman, Mol. Phys. 21 (1971) 1043.
[58] H. Sugihara, K. Shimokoshi, I. Yasumori, J. Phys. Chem. 81 (1977) 669.
[59] M.A. Spackman, H.P. Weber, J. Phys. Chem. 92 (1988) 794.
[60] Y.Y. Huang, J.E. Benson, M. Boudart, Ind. Eng. Chem. Fundam. 8 (1969) 346.
[61] E. Dempsey, in Molecular Sieves, Society of Chemical Industry, London, 1968, p. 293.
[62] E. Preuss, G. Linden, M. Peuckert, J. Phys. Chem. 89 (1985) 2955.
[63] J.C. White, J.B. Nicholas, A.C. Hess, J. Phys. Chem. B 101 (1997) 590.
[64] F. Blatter, H. Frei, to be submitted.
[65] M.V. Barnabas, A.D. Trifunac, Chem. Phys. Lett. 193 (1992) 298.
[66] S.W. Benson, Thermochemical Kinetics, Wiley, New York, 1968, p. 204.
[67] F. Blatter, H. Sun, H. Frei, Catal. Lett. 35 (1995) 1.
[68] H. Sun, F. Blatter, H. Frei, J. Am. Chem. Soc. 116 (1994) 7951.
[69] H. Sun, H. Frei, to be submitted.
[70] H. Sun, F. Blatter, H. Frei, J. Am. Chem. Soc. 118 (1996) 6873.
[71] F. Blatter, H. Sun, H. Frei, Chem. Eur. J., 2 (1996) 385; Angew Chem., Int. Ed. Engl., 35 (1996).
[72] H. Sun, F. Blatter, H. Frei, Catal. Lett. 44 (1997) 247.
[73] M. Iwasaki, K. Toriyama, K. Nunome, J. Am. Chem. Soc. 103 (1981) 3591.
[74] J. March, Advanced Organic Chemistry, 4th ed., Wiley, New York, 1992, p. 1099.
[75] S. Korcek, J.H.B. Chenier, J.A. Howard, K.U. Ingold, Can. J. Chem. 50 (1972) 2285.
[76] J. Datka, J. Chem. Soc., Farad. Trans. 1(77) (1981) 1309.
[77] S.M. Auerbach, N.J. Henson, A.K. Cheetham, H.I. Metiu, J. Phys. Chem. 99 (1995) 10600.
[78] J. Kärger, D.M. Ruthven, Diffusion in Zeolites, Wiley, New York, 1992, p. 459.
[79] S. Yashonath, J.M. Thomas, A.K. Novak, A.K. Cheetham, Nature 331 (1988) 601.
[80] A.A. Ukharskii, A.A. Kadushin, O.V. Al'tshuler, I.L. Tsitovskaya, Isv. Akad. Nauk. SSSR, Ser. Khim., (1975) 765.
[81] D.L. Vanoppen, D.E. De Vos, P.A. Jacobs, in: H. Chon, S.K. Ihm. Y.S. Uh (Eds.) Progress in zeolite and Microporous Materials studies in Surface Science and Catalysis, Vol. 105, Elsevier, Amsterdam, 1996.
[82] V. Balzani, F. Scandola, Supramolecular Photochemistry, Ellis Horwood, New York, 1991.
[83] N.J. Turro, J. Photochem. Photobiol. A: Chemistry 100 (1996) 53.
[84] H. Sun, H. Frei, J. Phys. Chem. B 101 (1997) 205.